Frequency encoding in excitable systems with applications to calcium oscillations

(calcium channels/mathematical model/inositol 1,4,5-trisphosphate)

YUANHUA TANG* AND HANS G. OTHMER†

*Department of Physiology and Biophysics, Cornell University Medical College, New York, NY 10021; and †Department of Mathematics, University of Utah, Salt Lake City, UT 84112

ABSTRACT **A number of excitable cell types respond to a constant hormonal stimulus with a periodic oscillation in intracellular calcium. The frequency of oscillation is often proportional to the hormonal stimulus, and one says that the stimulus is frequency encoded. Here we develop a theory of frequency encoding in excitable systems and apply it to intracellular calcium oscillations that result from increases in the intracellular level of inositol 1,4,5-trisphosphate.**

Cytoplasmic calcium (Ca hereafter) is a second messenger in many signal transduction processes. In recent years it has been found that Ca-based systems show a rich variety of dynamics in response to constant stimuli, including excitability, oscillations, and traveling Ca waves (1, 2). In some systems the response involves spikes whose frequency is proportional to the input stimulus. In the study of Ca dynamics in hepatocytes, Woods *et al.* (3) found that over the range of 200 nM to 1 μM in the concentration of vasopressin, constant stimuli evoke repetitive spikes in Ca concentration rather than simply elevating the level of Ca. Moreover, they found that as the hormone concentration was raised, the frequency of spiking increased but the amplitude remained nearly constant. Thus the continuously graded (analog) extracellular hormone signal was converted into a frequency-encoded digital signal (the number of Ca spikes).

Many types of cells transduce the amplitude of a stimulus into a frequency of Ca oscillations in response to a variety of stimulatory signals. For example, the oscillation frequency in hepatocytes is regulated by phenylephrine, angiotensin II, endothelin 1, glucagon, and ATP (3–5). Frequency encoding has also been found in endothelial cells in response to histamine and fluid shear stress (6), in mesangial cells in response to vasopressin, and in hair cells of the ear in response to pressure (7). Since similar dynamic behavior has been found in numerous cell types, it has been suggested that Ca spiking and frequency encoding may have a physiological role (8).

Consider an excitable system described by equations of the form

$$\varepsilon \frac{dx}{dt} = f(x, y, p)$$

$$\frac{dy}{dt} = g(x, y, p). \qquad [1]$$

Here $x \in R$, $y \in R$, $p \in R^k$ is a parameter vector, and ε is a small positive number. We suppose that f and g are smooth and defined everywhere in R^2 and a specified subset of the parameter space R^k. We further suppose that $f = 0$ can be solved for y in the form $y = F(x, p)$, where F is "cubic-like" in x in the sense that it has exactly one minimum at x_0, one maximum at x_1, and

$x_0 < x_1$. Finally we suppose that $g = 0$ can be solved for y in the form $y = G(x, p)$, that G is monotone increasing in x, and that the graph of G intersects $f = 0$ exactly once (Fig. 1). Many models of oscillatory or excitable systems that arise in physics, chemistry, and biology can be written in the form of Eqs. 1 (cf. ref. 9).

When $y = G(x, p)$ intersects $y = F(x, p)$ at $x < x_0$, the rest point (x_s, y_s) is stable, and when it lies sufficiently close to the minimum in $y = F$, the system is excitable. On the other hand, when the rest point lies between the minimum and the maximum and ε is sufficiently small, Eqs. 1 have a periodic solution. Finally, when $g = 0$ intersects $f = 0$ to the right of the maximum, the system is overstimulated and the rest point becomes stable again.

To understand how spiking above a baseline level of Ca occurs, suppose that the constant stimulus leaves $f = 0$ fixed but moves $g = 0$ so that the rest point lies on the ascending branch of $f = 0$. If ε is sufficiently small, the oscillations are composed of a rapid horizontal "upstroke" in x, a slow decrease of x and increase of y along the right branch of $f = 0$ (the excited state), a rapid horizontal "downstroke" of x, and a slow increase in x and decrease of y during the recovery phase. Such solutions are called relaxation oscillations or "spikes." Frequency encoding will result if the input simply multiplies both f and g, which is equivalent to scaling the time in proportion to the input. An increased frequency of the periodic solutions to increased stimuli may also result from scaling the slow dynamics, since the time the system spends in the upstroke and downstroke is very small. This is the second mode of frequency encoding. In addition, we may scale only one portion of the slow dynamics, for example, in the region of $x < x_0$ (Fig. 1) to scale the recovery time. In this case the overall shape of the spike is not changed, but the time spent in the recovery phase is reduced. These possibilities will be analyzed in the following sections.

The Mathematical Aspect of Frequency Encoding

We will call Eqs. 1 the *nondegenerate* system; the corresponding *degenerate* system is obtained by setting $\varepsilon = 0$.

$$0 = f(x, y, p)$$

$$\frac{dy}{dt} = g(x, y, p). \qquad [2]$$

By hypothesis the first equation in Eqs. 2 defines a curve Γ in the R^2 plane, and we assume that $(f_x(x, y, p))^2 + (f_y(x, y, p))^2 > 0$ on Γ. A point is called regular if $f_x(x, y, p) \neq 0$ and otherwise it is a nonregular point. We assume that the nonregular points on Γ are isolated and that for any nonregular point $f_{xx}(x, y, p) \neq 0$. In case a point is regular, we can locally

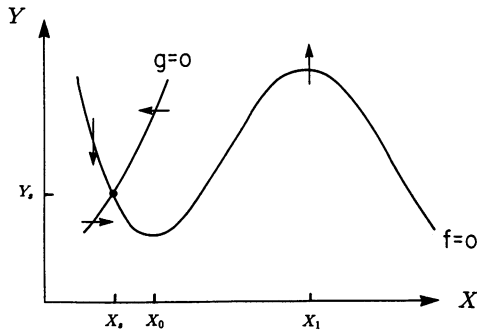Abbreviations: IP$_3$, inositol 1,4,5-trisphosphate; ER, endoplasmic reticulum.

FIG. 1.   Schematic of the isoclines $f = 0$ and $g = 0$ for a typical excitable system.

express the curve as $x = X(y, p)$. If a branch of Γ is composed of only regular points and $f_x(x, y, p) < 0$, this branch is called stable. Discontinuous solutions of Eqs. 2 can be constructed by patching together instantaneous jumps between stable branches and slow motion along the stable branches. The transition between stable branches occurs at the junction points where $f_x(x_0(y, p), y, p) = 0$ (see ref. 10). If a discontinuous solution forms a closed orbit Z_0 in the (x, y) plane, then Z_0 is called a discontinuous periodic solution of Eqs. 2. The period of this periodic solution is $T(0) = \oint_{Z_0} dy/g(x, y, p)$.

THEOREM 1. *Suppose that Eqs. 2 have a closed orbit Z_0 and the above-mentioned regularity conditions are satisfied. Then for sufficiently small ε, the nondegenerate system (Eqs. 1) has a unique and stable limit cycle Z_ε, which uniformly approaches Z_0 as $\varepsilon \to 0$. In addition, the period of Z_ε is $T(\varepsilon) = T(0) + \alpha\varepsilon^{2/3} + o(\varepsilon^{2/3})$, where α is a constant.*

A proof of this theorem is given in ref. 10. The approximation of the periodic solution to Z_0 is of order ε on the stable branches away from junction points and of order ε^a for the fast motion part, where $a \geq 2/3$. In a neighborhood of the junction points, the approximation is of order ε^a for $a \geq 0$. This approximation is called the zeroth approximation. *Theorem 1* can be extended to the case in which x and y are both vector variables, provided some additional regularity assumptions are met (10). From this theorem, we have the following corollary.

COROLLARY 1. *Let ε_1 and ε_2 be small and $\varepsilon_M = max(\varepsilon_1, \varepsilon_2)$. If the degenerate system (Eqs. 2) has a closed orbit Z_0 and the conditions in* Theorem 1 *are satisfied, then (i) the nondegenerate system (Eqs. 1) has periodic solutions $\phi(t, \varepsilon_i)$ with period $T(\varepsilon_i)$, $(i = 1, 2)$; (ii) $|\phi(t, \varepsilon_1) - \phi(t, \varepsilon_2)| = o(1)$ for $0 \leq t \leq T$, where $T > 0$ is fixed; and (iii) $T(\varepsilon_1) - T(\varepsilon_2) = O((\varepsilon_M)^{2/3})$.*

Exact frequency encoding results when the input multiplies both f and g, since then it corresponds to a simple scaling of time with no change in the amplitude. In approximate frequency encoding, the amplitude changes little with the input, and the frequency is approximately proportional to the input. The fact that $T(0)$ is the dominant contribution to the period when $\varepsilon > 0$ is sufficiently small suggests that approximate frequency encoding will exist if the input scales the slow dynamics. To make this precise, suppose that h can be taken out of $g(x, y, p)$ as a multiplicative factor—i.e., $g(x, y, p) = h\bar{g}(x, y, \bar{p})$. All other parameters are assumed to be fixed, and we suppose that h does not appear in $f(x, y, p)$. In this case *Corollary 1* implies the following result.
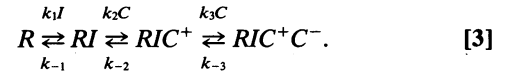
THEOREM 2. *Suppose that the conditions in* Theorem 1 *are satisfied and suppose that Eqs. 2 have a periodic solution $\phi(t, h_0, \varepsilon)$ of period $T(h_0, \varepsilon)$ for $h = h_0$ and $\varepsilon > 0$. Further, suppose that $r = h/h_0$ is $O(1)$ and let $\varepsilon_M = max(\varepsilon h, \varepsilon h_0)$. Then for sufficiently small $\varepsilon_M > 0$, (i) Eqs. 1 have a periodic solution $\hat{\phi}(t, h, \varepsilon) = \phi(rt, h_0, r\varepsilon)$ with period $\hat{T}(h, \varepsilon) = T(rh_0, \varepsilon)$, (ii) $|\hat{\phi}(t/r, h, \varepsilon) - \phi(t, h_0, \varepsilon)| = o(1)$ for $0 \leq t \leq max(r\hat{T}(h, \varepsilon), T(h_0, \varepsilon))$, and (iii) $r\hat{T}(h, \varepsilon) - T(h_0, \varepsilon) = O(\varepsilon_M^{2/3})$.*

Finally, there are two other types of approximate frequency encoding, which are more difficult to quantify, but which may

be the most important ones from an experimental standpoint. In many systems described by equations like Eqs. 1, the periodic solutions are characterized by a short time spent in the excited state and a long time spent in the recovery state, due to a large difference in the speed on the right and left branch of $f = 0$ (see Fig. 1). If the input modulates the speed of recovery, then one can obtain approximate frequency encoding. Alternatively, approximate frequency encoding results if the speed of recovery is unchanged, but the length of the recovery period is decreased by shortening the left branch of $f = 0$. This alters the baseline level of the recovery variable, but the shape of the spikes is approximately unchanged, as in the above cases. Since the information is carried by the spikes, the end result of signal transduction is not affected. This type of approximate frequency encoding will be illustrated later in the context of the model for Ca oscillations.

A Four-State Model for Intracellular Ca Dynamics

A four-state model for the IP_3-sensitive Ca channel connecting the endoplasmic reticulum (ER) and the cytoplasm was proposed in ref. 1. The transitions between the different states occur according to the following scheme:

$$R \underset{k_{-1}}{\overset{k_1 I}{\rightleftarrows}} RI \underset{k_{-2}}{\overset{k_2 C}{\rightleftarrows}} RIC^+ \underset{k_{-3}}{\overset{k_3 C}{\rightleftarrows}} RIC^+C^-. \qquad [3]$$

Here R denotes the bare receptor for the IP_3-sensitive Ca channel, I denotes IP_3, C denotes the cytoplasmic Ca, RI denotes the receptor-IP_3 complex, and RIC^+ (RIC^+C^-) denotes RI with Ca bound at the activating site (the activating and inhibitory sites).

Let C_i be the dimensional Ca concentration in the cytoplasm, and let x_i, $i = 2, \ldots, 5$, denote the fractions in states R, RI, RIC^+, and RIC^+C^-, respectively. We assume that there is no exchange of Ca between the extracellular medium and the cytoplasm, which is a good approximation where Ca influx into the cell is small. We further assume that the conductivity of the IP_3-sensitive channel is a linear function of the fraction of channels open, and we suppose that the rate that reloads the ER is described by a Hill function with coefficient 2. Then the governing equations for Ca and the channel fractions are as follows (cf. ref. 1):

$$\frac{dC_i}{dt} = (1 + v_r)(g_0 + g_1 x_4)(C_M - C_i) - v_r \frac{p_1 C_i^2}{C_i^2 + p_2^2}$$

$$\frac{dx_2}{dt} = -k_1 I x_2 + k_{-1} x_3$$

$$\frac{dx_3}{dt} = -(k_{-1} + k_2 C_i)x_3 + k_1 I x_2 + k_{-2} x_4 \qquad [4]$$

$$\frac{dx_4}{dt} = -(k_{-2} + k_3 C_i)x_4 + k_2 C_i x_3 + k_{-3} x_5$$

$$\frac{dx_5}{dt} = k_3 C_i x_4 - k_{-3} x_5.$$

Here v_r is the ratio of the ER volume to the cytoplasmic volume, and C_M is the volumetric average Ca concentration. The parameter values used are listed in Table 1. This set of parameters differs from the set estimated in ref. 1, but the rates used here are consistent with the known equilibrium data and they lead to a sharper separation between the slow and fast dynamics in the system.

We introduce new dimensionless variables $\tau = t \cdot k_{-3}$, $y = x_5$, and $x = C_i/C_M$ and use the fact that $\Sigma_{i=2}^{5} x_i = 1$ to reduce Eqs. 4 to

Physiology: Tang and Othmer

Proc. Natl. Acad. Sci. USA 92 (1995)   7871

Table 1. Dimensional parameters and their values

Constant	Definition	Value
v_r	ER volume/cytoplasmic volume	0.185
g_0	Leakage coefficient	0.025 s^{-1}
g_1	Channel conductance	36.0 s^{-1}
p_1	Maximum pump rate	54.0 μM·s^{-1}
p_2	Michaelis constant	0.03 μM
C_M	Average Ca concentration	1.56 μM
k_1	IP$_3$ on rate	120.0 μM^{-1}·s^{-1}
k_2	On rate for activation	150.0 μM^{-1}·s^{-1}
k_3	On rate for inhibition	0.18 μM^{-1}·s^{-1}
k_{-1}	IP$_3$ off rate	96.0 s^{-1}
k_{-2}	Off rate for activation	18.0 s^{-1}
k_{-3}	Off rate for inhibition	0.018 s^{-1}

Table 2. Definition of the dimensionless parameters and their values

Parameter	Definition	Value
ε_1	$\dfrac{k_{-3}}{k_{-1}}$	1.88×10^{-4}
ε_2	$\dfrac{k_{-3}}{k_{-2}}$	1.0×10^{-3}
ε	$\dfrac{k_{-3}C_M}{v_r p_1}$	2.81×10^{-3}
α_1	$\dfrac{(1 + v_r)C_M g_0}{v_r p_1}$	4.63×10^{-3}
α_2	$\dfrac{(1 + v_r)C_M g_1}{v_r p_1}$	6.66
α_3	$\dfrac{p_2}{C_M}$	0.019
$\beta_0(I)$	$\dfrac{k_{-1}}{k_1 I}$	0.8/I
β_1	$\dfrac{k_{-2}}{k_2 C_M}$	0.077
β_2	$\dfrac{k_3 C_M}{k_{-3}}$	15.625
β_3	$\dfrac{k_{-1}}{k_{-2}}$	5.33

$$\varepsilon \frac{dx}{d\tau} = (\alpha_1 + \alpha_2 x_4)(1 - x) - \frac{x^2}{x^2 + \alpha_3^2}$$

$$\frac{dy}{d\tau} = \beta_2 x(1 - x_2 - x_3 - y) - y$$

$$\varepsilon_1 \frac{dx_2}{d\tau} = -\frac{x_2}{\beta_0(I)} + x_3 \qquad [5]$$

$$\varepsilon_2 \frac{dx_3}{d\tau} = -\beta_3\left(x_3 - \frac{x_2}{\beta_0(I)}\right) - \frac{x_3 x}{\beta_1} + x_4,$$

where the definitions of dimensionless parameters and their values are listed in Table 2. The binding and release of IP$_3$ at the IP$_3$ site and the binding and release of Ca at the activating site on the channel are rapid compared with the binding and release of Ca at the inhibitory site. Thus ε_1 and ε_2 are small and we may formally set them to zero to obtain

$$x_2 = \frac{\beta_0(I)\beta_1(1 - y)}{x + \beta_1(1 + \beta_0(I))}$$

$$x_3 = \frac{\beta_1(1 - y)}{x + \beta_1(1 + \beta_0(I))} \qquad [6]$$

$$x_4 = \frac{x(1 - y)}{x + \beta_1(1 + \beta_0(I))}.$$

The remaining differential equations are

$$\varepsilon \frac{dx}{d\tau} = \alpha_1(1 - x) + \alpha_2(1 - x)\frac{x(1 - y)}{x + \beta_1(1 + \beta_0(I))} - \frac{x^2}{x^2 + \alpha_3^2}$$

$$\frac{dy}{d\tau} = -y + \frac{\beta_2 x^2(1 - y)}{x + \beta_1(1 + \beta_0(I))}. \qquad [7]$$

Thus the system for intracellular Ca dynamics with an IP$_3$-sensitive channel has the same form as Eqs. 1. Moreover, the nullclines are similar to those for a typical excitable system shown in Fig. 1 (compare with Fig. 2). Also shown in Fig. 2 is a periodic solution, and the time course of the Ca component for this solution is shown in Fig. 3.

This simple system not only reproduces all the experimentally observed phenomena qualitatively but it can also simulate most of these results quantitatively. For example, the steady-state fraction of open channels as a function of pCa is a bell-shaped curve, and the parameter values used here predict the experimental results very well. When a step change in Ca is applied to the channel equations, the fraction of channels in the open state (x_4) shows partial adaptation (11). The complete model simulates the excitability to pulses of Ca or IP$_3$ at low IP$_3$ levels and results in Ca oscillations when the IP$_3$ concen-

tration lies in a suitable range. The recovery of excitability is due to the recovery of the channel from the inhibited state, rather than to restoration of Ca. The Ca oscillations have the property of frequency encoding as the IP$_3$ concentration is varied, which will be investigated in the following section. When the IP$_3$ concentration exceeds a certain level, the periodic solutions disappear and the system remains at a sustained high level of cytoplasmic Ca. The transitions from excitable responses to oscillations and from oscillations to a high level of cytoplasmic Ca can be easily understood by studying the null clines in the phase plane. As the IP$_3$ level increases, the steady-state solution at the intersection of the null clines goes from stable, to unstable, and to stable again as IP$_3$ increases. A computer simulation of several types of behavior of this system is shown in Fig. 4. This simulation matches the experimental data obtained from endothelial cells well (6).

Frequency Encoding in the Model System

As we remarked earlier, we get exact frequency encoding if the input scales the time, and this would occur in the present model if IP$_3$ scaled the off rate k_3. However, this is not the case, nor
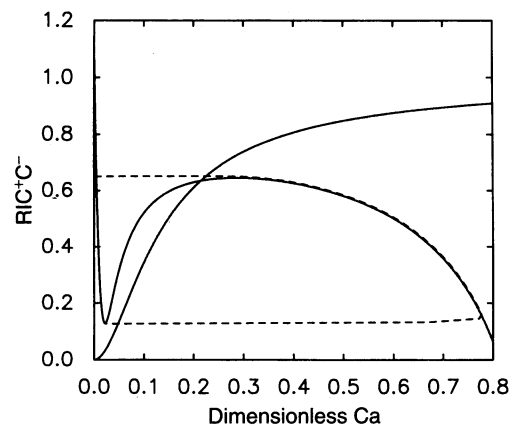

FIG. 2. Null clines (solid lines) and a periodic solution (dashed line) of Eqs. 1 for IP$_3$ = 0.5 μM.
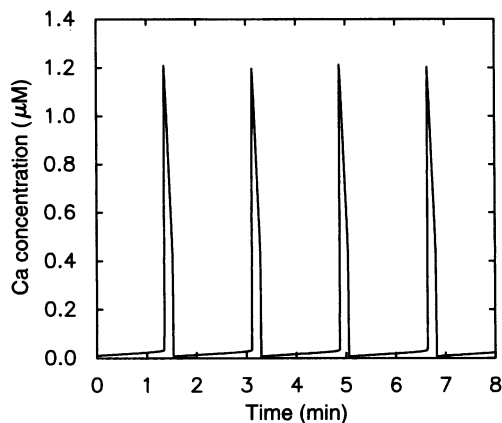
FIG. 3. The time course of the Ca component of the periodic solution shown in Fig. 2.

is there a scaling for which this is true. We can obtain approximate frequency encoding by introducing a multiplicative factor h on the right hand side of Eqs. **7**. According to *Theorem 2*, if we scale h by a factor of r, the period of the oscillations will change by a factor of approximately $1/r$. This is illustrated in Fig. 5. By comparing Figs. 3 and 5, we see that as h increases the period decreases. The width of the Ca spike changes as well, since the time scale is altered in both the excited and the recovery phase.

Although we are able to obtain frequency encoding through changes in h, h is an artificially introduced factor and there is no uniform multiplicative factor for the slow dynamics that is modulated by IP$_3$ directly. Yet we see from Fig. 4 that the model exhibits frequency encoding, and to determine how well it does, we have computed the solution over the entire oscillatory range. In Fig. 6 we display the Ca concentration and the period of the oscillations as a function of IP$_3$ concentration. We see that the amplitude only changes by 20% over a wide range of IP$_3$ concentrations, whereas the period changes 10-fold. This indicates that frequency encoding arises via the third mode identified earlier—namely, via modulation of the dynamics in the recovery phase. In principle such modulation could occur either via a change in the speed on the slow branch or by changing the length of the slow branch, or both. To understand which occurs in this system, we display the null clines as a function of IP$_3$ in Fig. 7. We see that the length of the slow branch changes dramatically with the change in IP$_3$, whereas a multiplicative factor on the slow dynamics would not alter the null clines. We can also see here that the peak of cytoplasmic Ca will decrease slightly and the basal level will
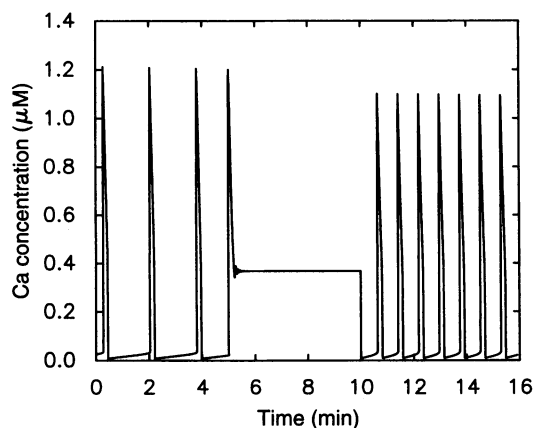
increase slightly in this mode of frequency encoding. The latter fact is what is observed experimentally in ref. 12.

We can qualitatively understand why the slow branch changes as follows. As the IP$_3$ level increases, the number of channels in the RI and RIC^+ state increases in the recovery phase, which leads to a higher basal level of cytoplasmic Ca. This increased basal level means that less additional RIC^+ is needed to trigger the positive feedback loop that produces the Ca increase and that Ca can increase ($f > 0$) at a larger value of RIC^+C^-. These two aspects are reflected in the null cline of $dx/dt = 0$ in Fig. 7 as (i) a rightward shift of the minimum; and (ii) the upward shifting of the minimum, as the IP$_3$ level increases. This upward shift decreases the recovery time and leads to frequency encoding.

Discussion

We have shown that there are three distinct modes by which frequency encoding can arise in excitable systems. The last two, which are the important ones, are based on modulating the slow dynamics of the system. The second mode is via a uniform modulation of the speed of the slow dynamics in both the excited and the recovery phase, while the third only involves a modulation of the time spent in the recovery phase. In the third mode the amplitude and width of the spike is essentially unchanged. In each case, the frequency modulation is accomplished by changing a single parameter in the system.

In the model for Ca dynamics analyzed here, frequency encoding in IP$_3$-regulated Ca oscillations is of the third type. Only one branch of the null cline for the fast dynamics is shortened significantly by a change in the frequency encoding parameter, the IP$_3$ concentration; the other branch is affected very little. As a result, the time course of the excited phase is
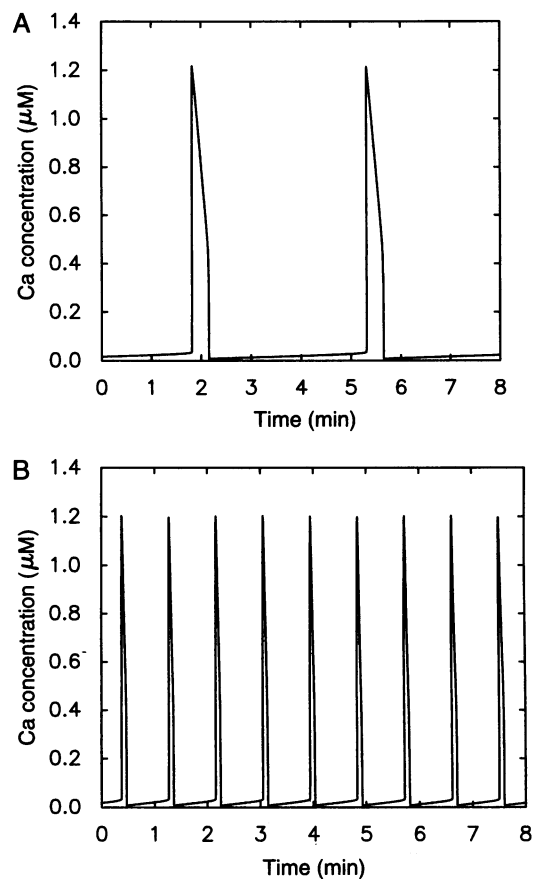

FIG. 5. Frequency encoding due to changes in the scale factor h for fixed IP$_3$ = 0.5 μM. (*A*) h = 0.5. (*B*) h = 2.0.
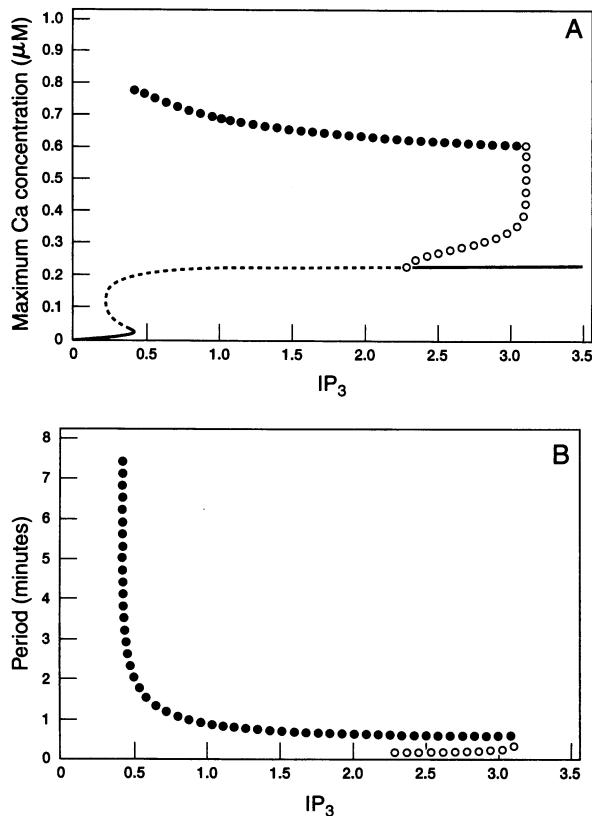

FIG. 4. Simulation of the response to a time-dependent level of IP$_3$. The IP$_3$ concentration was held at 0.5 μM for $t \in (0, 5)$, at 2 μM for $t \in (5, 10)$, and at IP$_3$ = 1.0 μM thereafter.

Physiology: Tang and Othmer

Proc. Natl. Acad. Sci. USA 92 (1995)   7873

FIG. 6.   Ca concentration (A) and period (B) as a function of IP$_3$ concentration (μM). A solid (dashed) line denotes a stable (unstable) steady state, and a solid (open) circle denotes a stable (unstable) periodic solution. In A the maximum Ca value on the orbit is shown for periodic solutions.

essentially unaltered and the recovery phase is compressed with increasing IP$_3$. The minimum Ca concentration reached is raised as the IP$_3$ level increases in this case. This differs from the first two modes of frequency encoding, in which the minimum level of Ca is unaltered by changes in the input parameter.
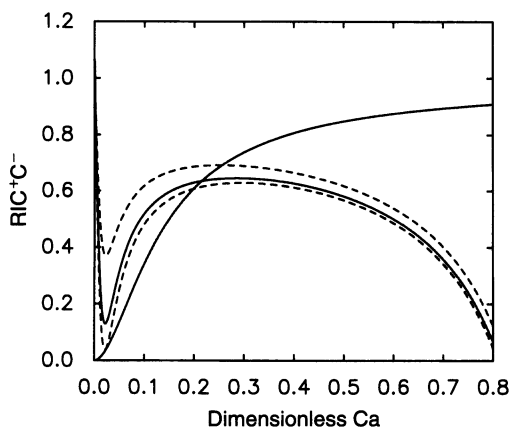

FIG. 7.   Null clines of Eqs. 7 for different values of IP$_3$. For the f = 0 null cline, the solid line corresponds to IP$_3$ = 0.5 μM, and the dashed lines correspond to IP$_3$ = 1.0 μM (upper curve) and IP$_3$ = 0.42 μM (lower curve). For the curve g = 0, only IP$_3$ = 0.5 μM is shown; the other two curves (IP$_3$ = 0.42 μM, IP$_3$ = 1.0 μM) are very close to this one.

Ca dynamics in hepatocytes has served as a model system for experimental studies on frequency encoding (3, 13, 14). As a stimulus is increased, the frequency of oscillation can increase more than 20-fold, while the change in amplitude is minimal. A typical duration of the Ca spike in response to agonists is about 7 sec (3), despite the fact that the period may vary from 210 sec to 10 sec (15). Furthermore, for certain hormones the time course of an individual spike is essentially unchanged over wide ranges of the stimulus (16, 17). In addition, there is an increase in the basal Ca level as the oscillation frequency increases (12). These observations demonstrate that frequency encoding in hepatocytes in response to certain agonists is of the third type of frequency encoding identified in this paper. The simplified model represents the above-mentioned phenomena very well.

Experiments show that there may be two types of Ca stores in hepatocytes, one IP$_3$-sensitive and possibly a ryanodine-sensitive one (18, 19). Different hormones may interact with either one or both Ca stores to mediate intracellular Ca variations (5). The exact nature of the interaction between the two stores is unclear. This restricts the application of our model to study frequency modulations if both the IP$_3$-sensitive and the ryanodine-sensitive Ca stores are involved. However, the model is appropriate, at least for the cases when only the IP$_3$-sensitive Ca store is involved. The Ca oscillations in response to phenylephrine is one such case, since the dynamics are not affected by ryanodine in this case (16).

1. Othmer, H. G. & Tang, Y. (1993) in *Experimental and Theoretical Advances in Pattern Formation*, eds. Othmer, H. G., Maini, P. K. & Murray, J. D. (Plenum, New York), pp. 277–313.
2. Berridge, M. J. (1993) *Nature (London)* **361**, 315–325.
3. Woods, N. M., Cuthbertson, K. S. R. & Cobbold, P. H. (1986) *Nature (London)* **319**, 600–602.
4. Somogyi, R., Zhao, M. & Stucki, J. W. (1992) *Biochem. J.* **286**, 869–877.
5. Sanchez-Bueno, A., Marrero, I. & Cobbold, P. (1993) *Biochem. J.* **291**, 163–168.
6. Jacob, R., Merritt, J. E., Hallam, T. J. & Rink, T. J. (1988) *Nature (London)* **335**, 40–45.
7. Alberts, B., Bray, D., Lewis, J., Raff, M., Roberts, K. & Watson, J. (1989) *Molecular Biology of the Cell* (Garland, New York), 2nd Ed.
8. Meyer, T. & Stryer, L. (1991) *Annu. Rev. Biophys. Biophys. Chem.* **20**, 153–174.
9. Alexander, J. C., Doedel, E. J. & Othmer, H. G. (1990) *SIAM J. Appl. Math.* **50**, 1373–1418.
10. Mishchenko, E. F. & Rosov, N. K. (1980) *Differential Equations with Small Parameters and Relaxation Oscillations*, Mathematical Concepts and Methods in Science and Engineering (Plenum, New York).
11. Tang, Y. & Othmer, H. G. (1994) *Biophys. J.* **67**, 2223–2235.
12. Hajjar, R. & Bonventre, J. (1991) *J. Biol. Chem.* **266**, 21589–21594.
13. Rooney, T. A., Sass, E. J. & Thomas, A. P. (1989) *J. Biol. Chem.* **264**, 17131–17141.
14. Schofl, C., Brabant, G., Hesch, R., von Muhlen, A., Cobbold, P. & Cuthbertson, K. (1993) *Am. J. Physiol.* **265**, C1030–C1036.
15. Woods, N., Cuthbertson, K. & Cobbold, P. (1987) *Biochem. J.* **246**, 619–623.
16. Sanchez-Bueno, A. & Cobbold, P. (1993) *Biochem. J.* **291**, 169–172.
17. Tanaka, Y., Hayashi, N., Kaneko, A., Ito, T., Miyoshi, E., Sasaki, Y., Fusamoto, H. & Kamada, T. (1992) *Hepatology* **16**, 479–486.
18. Osada, S., Okano, Y., Saji, S. & Nozawa, Y. (1994) *Hepatology* **19**, 514–517.
19. Rooney, T. A., Renard, D. C., Sass, E. J. & Thomas, A. P. (1991) *J. Biol. Chem.* **266**, 12272–12282.